Ther Adv Gastroenterol
2020, Vol. 13: 1–12
DOI: 10.1177/1756284820969050

Four-dimensional impedance manometry derived from esophageal high-resolution impedance-manometry studies: a novel analysis paradigm

Wenjun Kou, Dustin A. Carlson, Neelesh A. Patankar, Peter J. Kahrilas and John E. Pandolfino

Abstract

Background: This study aimed to introduce a novel analysis paradigm, referred to as 4-dimensional (4D) manometry based on biophysical analysis; 4D manometry enables the visualization of luminal geometry of the esophagus and esophagogastric junction (EGJ) using high-resolution-impedance-manometry (HRIM) data.

Methods: HRIM studies from two asymptomatic controls and one type-I achalasia patient were analyzed. Concomitant fluoroscopy images from one control subject were used to validate the calculated temporal-spatial luminal radius and time-history of intraluminal bolus volume and movement. EGJ analysis computed diameter threshold for emptying, emptying time, flow rate, and distensibility index (DI), which were compared with bolus flow time (BFT) analysis.

Results: For normal control, calculated volumes for 5 ml swallows were 4.1 ml–6.7 ml; for 30 ml swallows 21.3 ml–21.8 ml. With type-I achalasia, >4 ml of intraesophageal bolus residual was present both pre- and post-swallow. The four phases of bolus transit were clearly illustrated on the time-history of bolus movement, correlating well with the fluoroscopic images. In the control subjects, the EGJ diameter threshold for emptying was 8 mm for 5 ml swallows and 10 mm for 30 ml swallows; emptying time was 1.2–2.2 s for 5 ml swallows (BFT was 0.3–3 s) and 3.25–3.75 s for 30 ml swallows; DI was 2.4–3.4 mm^2/mmHg for 5 ml swallows and 4.2–4.6 mm^2/mmHg for 30 ml swallows.

Conclusions: The 4D manometry system facilitates a comprehensive characterization of dynamic esophageal bolus transit with concurrent luminal morphology and pressure from conventional HRIM measurements. Calculations of flow rate and wall distensibility provide novel measures of EGJ functionality.

Keywords: 4D manometry, esophagus, esophageal manometry, intraluminal impedance, peristalsis

Received: 21 May 2020; revised manuscript accepted: 24 August 2020.

Correspondence to:
Wenjun Kou
Feinberg School of medicine, Northwestern University, 676 North Saint Clair Street, Chicago, IL 60611, USA
w-kou@northwestern.edu

Dustin A. Carlson
Peter J. Kahrilas
John E. Pandolfino
Feinberg School of Medicine, Northwestern University, Chicago, IL, USA

Neelesh A. Patankar
Department of Mechanical Engineering, Northwestern University, Evanston, IL, USA

Introduction

The primary function of the esophagus is to transport ingested food from the mouth to the stomach utilizing delicately balanced neuromuscular control and biomechanical tissue properties. This manifests as temporal-spatial variation of esophageal wall morphology, stress, and luminal pressure during bolus transit.[1–3] Consequently, extracting the details of esophageal pressurization with concurrent luminal morphology is crucial for the understanding and management of esophageal dysfunction. Currently, the dominant technology utilized in the assessment of esophageal motility is high-resolution manometry (HRM) along with

the Chicago Classification,[4] but this falls short in assessing the corresponding aberrations in esophageal morphology. Hence, intraluminal ultrasound, concomitant fluoroscopy, computed tomography, and magnetic resonance imaging have been utilized experimentally to enhance the assessment of esophageal luminal geometry.[5–9] However, for technical and practical reasons, none of these have been applied widely.

High-resolution impedance manometry (HRIM) offers an alternative strategy to simultaneously monitor intraluminal pressure and luminal geometry. The functional luminal imaging probe (FLIP) dynamically monitors luminal geometry within a cylindrical bag of conducting fluid but provides limited intraluminal pressure resolution.[10,11] HRIM integrates high-resolution pressure and impedance measurement into a single catheter but, thus far, has suffered from a very limited, dichotomous analysis of bolus present/bolus absent assessment with respect to the impedance data.[12,13] However, HRIM, could offer truly concurrent temporal-spatial dynamics of luminal geometry and pressure with more sophisticated analysis techniques. In this work, we propose such a biophysical analysis technique, referred to as 4-dimensional (4D) manometry assessing HRIM data dynamically along the dimensions of pressure, cross-sectional area, esophageal length, and time. We hypothesize that the proposed 4D manometry analytic technique could extract comprehensive details of esophageal morphology and pressurization and enable subsequent analysis of bolus flow rate, flow velocity, and distensibility index (DI) of the esophageal-gastric junction (EGJ) during esophageal emptying using only conventional HRIM data. Thus, the goal of the current study was to introduce 4D manometry methodology and evaluate its efficacy in extracting biophysical information. Also included was a preliminary validation of this technique.

Materials and methods

Subjects

The 4D manometry analysis paradigm was developed and tested by comparison with concurrent fluoroscopic imaging, bolus flow time (BFT) analysis, and distensibility analysis obtained from a FLIP study. Three cases were analyzed: (1) an asymptomatic control with concurrent HRIM and fluoroscopy studied in our previous report referred to as *Control 1*[6]; (2) a second asymptomatic control studied with HRIM and FLIP varying the bolus volume and constituents during the HRIM study, referred to as *Control 2*; and (3) a type-I achalasia patient studied with HRIM and FLIP, referred to *Type-I Ach*.

The study protocol was approved by the Northwestern University Institutional Review Board (STU00096856, approved November 2014). Informed consent was obtained from all subjects in a written format; control subjects were paid for their participation.

Study protocol

The HRIM catheter utilized was a 4.2-mm outer diameter solid-state assembly with 36 circumferential pressure sensors at 1-cm interval, and 18 impedance segments at 2-cm intervals (Given Imaging, Los Angeles, CA, USA). Transducers were calibrated at 0–300 mmHg using externally applied pressure. The assembly was placed transnasally and positioned to record from the hypopharynx to the stomach with about three intragastric pressure sensors. HRIM data and fluoroscopic imaging were acquired simultaneously using the HRIM video system (model A400, Given Imaging), which synchronized the fluoroscopic images with manometric data during acquisition. Fluoroscopy was performed with a multipurpose X-ray system (Artis MP, Siemens, Malvern, PA, USA). This information was then displaced on a computer screen in real time and stored on a hard drive for further analysis. The HRIM protocol included a first 5-min baseline recording and then 20-s to 30-s interval for each swallow. FLIP studies were done in conjunction with endoscopy. The 16-cm FLIP (EndoFLIP® EF-322N; Medtronic, Inc., Shoreview, MN, USA) was calibrated to atmospheric pressure prior to trans-oral probe placement. With the endoscope withdrawn, the FLIP was positioned within the esophagus such that 1–3 impedance sensors were observed beyond the EGJ with this positioning maintained throughout the FLIP study. Stepwise, 10-ml balloon distensions beginning with 20 ml and increasing to target volume of 70 ml were then performed; each stepwise distension volume was maintained for 30–60 s.

For Control 1, concurrent HRIM and videofluoroscopy were done during six barium swallows (5 ml of barium mixed with 50% normal saline) in

a supine position and four in an upright position after ⩾6-h fasting. For Control 2, 22 swallows were performed during HRIM procedure: 10 supine swallows of 5 ml 50% normal saline, 2 supine swallows of 5 ml 100% normal saline, and 10 upright swallows (5 of 5 ml 50% normal saline, 2 of 5 ml 100% normal saline, 2 of 30 ml 50% normal saline, and 1 multiple repetitive swallow that was not used in the analysis). The Type-I Ach subject was studied with 10 supine swallows and 5 upright swallows of 5 ml 50% normal saline.

4D manometry analysis

Overview of 4D manometry analysis. Similar to the previous BFT algorithm, the analysis was applied to each swallow for each case. A 30-s HRIM data block was imported from ManoView (Medtronic Inc.) including at least 3 s of pre-swallow baseline data into a customized MATLAB program along with notations of the upper esophageal sphincter (UES) channel number, crural diaphragm channel number, swallow start time, and swallow end time.

Simultaneous rendering of space-time variation of pressure, impedance, and esophageal luminal morphology. We first linearly interpolated the 18-channel impedance data to 36-channels to align the impedance and pressure data both temporally and spatially and plotted superimposed pressure and impedance color maps. We then identified three key landmarks: the UES channel, the lower esophageal sphincter (LES) channel, and the high-pressure zone channel number. The swallow starting time was identified in the UES channel and set as time 0 in the ensuing analysis. The swallow end time was based on LES restoration or at 12 s, based on our previous experience with BFT analysis. The time range of interest is from time –3 s to the swallow end time (see Figure 1). The spatial-temporal total conductance, $G(h,t)$ was obtained using the interpolated impedance data. Based on biophysical principles detailed in the Appendix, the spatial-temporal values of luminal liquid cross-sectional area (CSA), $CSA_l(h,t)$ was then obtained. Note that for a normal swallow with minimal pre-swallow residual, the mucosal conductance at channels above the LES, was computed as the minimal value of total conductance (see Appendix). The mucosal conductance of channels below the LES, where liquid potentially always exists, was approximated by the median of mucosal conductance in the esophageal body. For swallows with pre-swallow residual as with Type-I Ach, mucosal conductance at channels with non-zero residual could be approximated as the median of mucosal conductance at channels with minimal residual. See Appendix and Discussion for details.

With the spatial-temporal values of luminal liquid CSA, $CSA_l(h,t)$, the luminal radius at each time and channel, $R_{\text{lumen}}(h,t)$ was obtained based on catheter radius, R_{catheter}, assuming a circular lumen.

$$R_{\text{lumen}}(h,t) = \sqrt{\frac{CSA_l(h,t)}{\pi} + R_{\text{catheter}} \times R_{\text{catheter}}}$$

With the above data, a simultaneous rendering of space-time variation of pressure, impedance, and luminal morphology, along with the time-history of bolus volume, was generated (see supplemental movies).

Bolus transit analysis: quantifying time-history of bolus retention volume and bolus transit characteristics. At each instant, the channel with the maximal pressure along the esophageal body was identified as the contraction channel. The bolus retention volume was defined as the volume of liquid proximal to the contraction channel, and calculated by integrating bolus CSAs from the UES channel to the contraction channel at that instant. A time-history of bolus retention volume was then obtained. Similarly, the time-history of bolus volume within the esophageal body (i.e., above the crural diaphragm channel) was obtained and used to identify various phases of bolus transit. The emptying period was defined as the duration of the effective esophageal emptying (introduced later). The emptying flux across the EGJ was calculated as the change of esophageal bolus volume during emptying divided by the emptying time.

EGJ analysis: determining EGJ emptying period, flow characteristics, and distensibility

An EGJ region of interest (ROI) extended from 1 cm above the crural diaphragm line to 1 cm below the crural diaphragm line and from –3 s to 12 s. Pressure data and bolus CSA data within the ROI (three channels, respectively), were then plotted in

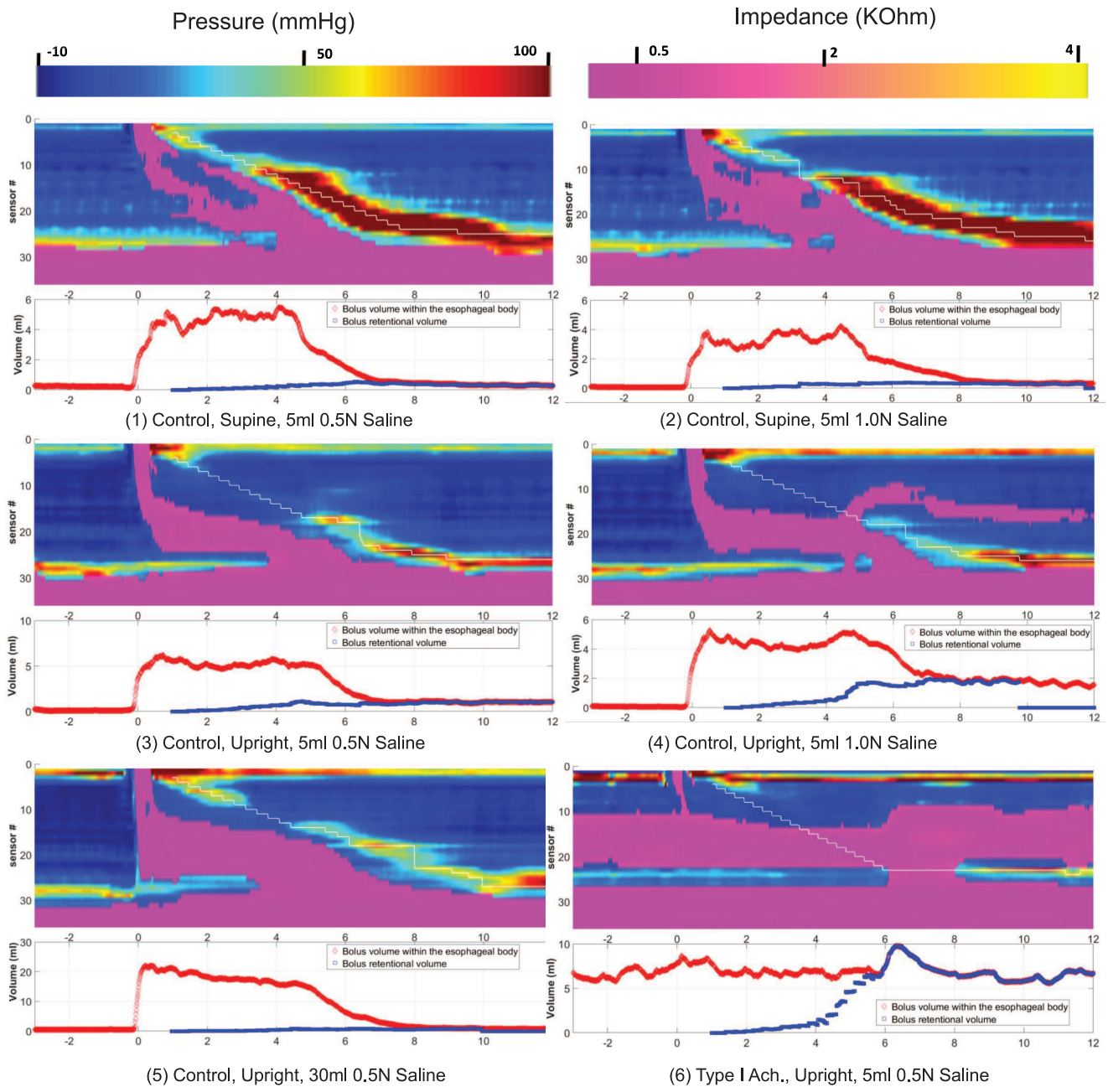

Figure 1. Pressure-impedance topography concurrent with bolus transit history of various swallows/cases. The bolus volume within the body is defined as the total calculated volume of liquid bolus between the UES and LES channels; the retention volume as the volume of liquid proximal to the CW channel but distal to the UES channel at each time.
CW, contraction wave; LES, lower esophageal sphincter; UES, upper esophageal sphincter.

conjunction with volume data for simultaneous analysis. An emptying diameter was introduced as the threshold diameter allowing bolus passage. The EGJ segment was defined as open when all the three channels within the ROI equaled or exceeded the emptying diameter. The chosen emptying diameter was validated during esophageal emptying using the corresponding bolus volume data, detailed in the EGJ analysis discussion.

The first validation included a comparison of calculated bolus volumes with the actual bolus volumes in Control 2. The second validation was based on the fluoroscopy study on Control 1

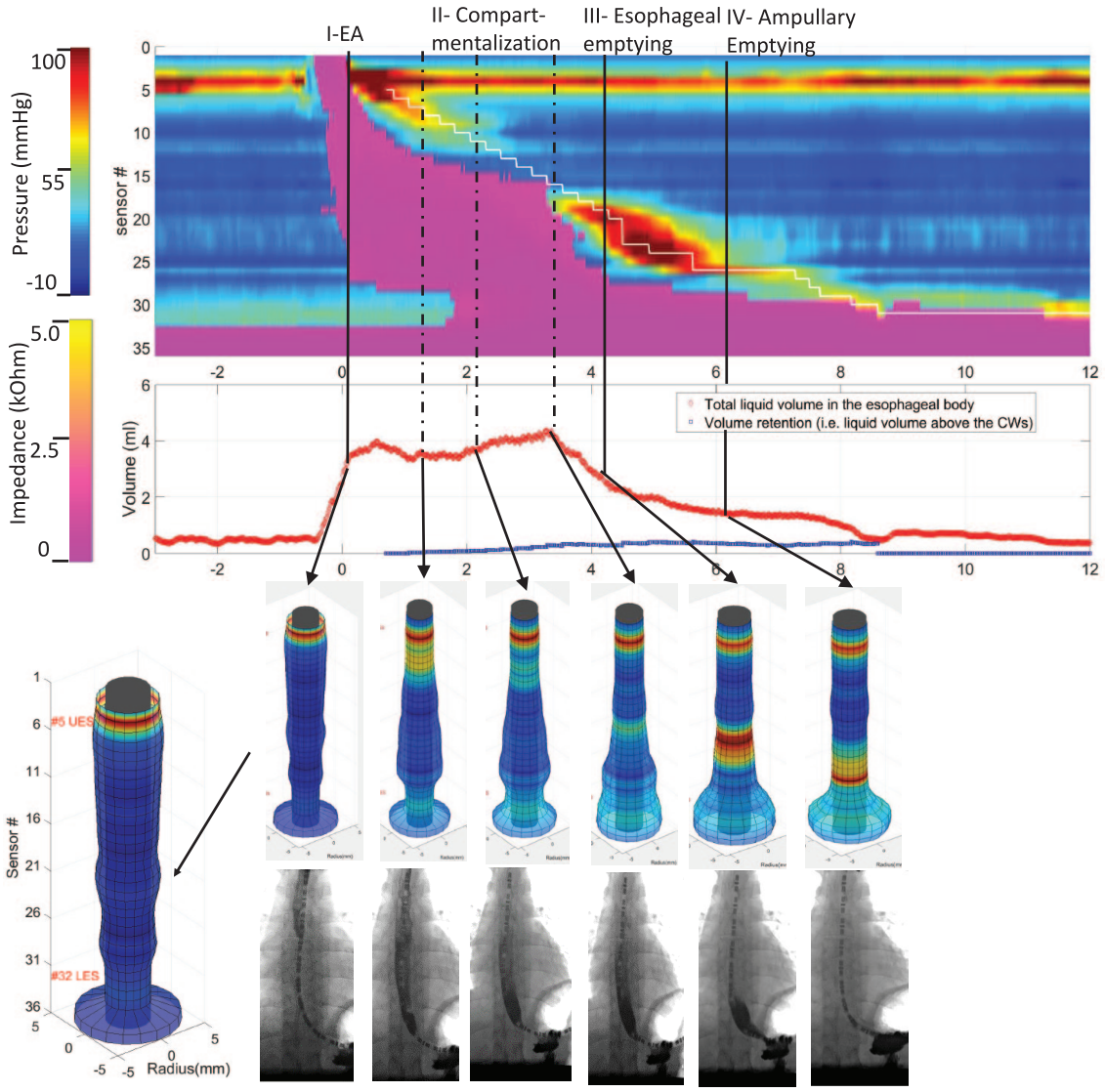

Figure 2. 4D manometry analysis on Control 1 against X-ray image to delineate bolus transit. (Top) A simultaneous plot of impedance, pressure, bolus volume, and retention volume history obtained by 4D manometry on Swallow #7 of Control 1. The delineation of the four-phases of bolus transit was illustrated based on bolus volume history. (Bottom) 3D rendering of esophageal luminal morphology corresponding to each phase, compared with the X-ray images below. Note that the lumen is simplified as a straight tube during the geometric construction.
3D, three-dimensional; 4D, four-dimensional.

which included 10 swallows of 5 ml mixture of barium and saline. The X-ray quality, however, was variable among swallows, such that swallow #7 was most suitable for detailed analysis to delineate the phases of bolus transit (see Figure 2).

We then focused on the EGJ analysis comparing the 4D manometry analysis with BFT, esophageal impedance integral (EII) ratio, and the DI from corresponding FLIP study in Control 2. To quantify the EGJ emptying from 4D manometry, the emptying diameter was first investigated. The onset of emptying occurred when bolus volume achieved its maximal value and the emptying diameter defined both the onset and offset of effective esophageal emptying as well as facilitating the quantification of EGJ flow. Once the period of esophageal emptying was identified, the emptying period (comparable with BFT), EGJ pressure, and EGJ diameter were extracted.

Table 1. Predicted bolus volume and EGJ flow onset time predicted from 4D manometry against nominal volume and fluoroscopic evaluation, respectively. Note that EGJ flow onset time was measured by the time lapse from swallow onset and was computed with two criteria from 4D manometry. One is based on onset of bolus volume decrease, referred to as Flow onset time (4D manometry: volume criterion) and the other uses onset of esophageal emptying based on diameter criteria, referred to as Flow onset time (4D manometry: diameter criterion). EGJ emptying diameter was chosen to be 8 mm and 10 mm, for 5 ml swallow and 30 ml swallow, respectively. Only the first case, Control 1, included concurrent fluoroscopic data.

	Bolus volume from 4D manometry (ml)	Flow onset time (s) (4D manometry: volume criterion)	Flow onset time (s) (4D manometry: diameter criterion)	Flow onset time (s) (fluoroscopy)
Control 1 Supine (5 ml)	5.6 (5.5–5.8)	4.4 (4.1–4.9)	3.8 (3.6–4.3)	3.3 (3.2–3.5)
Control 1 Upright (5 ml)	3.6 (3.2–4.0)	3.8 (3.6–3.9)	3.5 (3.2–3.8)	2.7 (2.4–3.0)
Control 2 Supine (5 ml) 0.5 *N* saline	5.7 (5.6–6.1)	4.2 (4.1–4.3)	4.3 (4.1–4.3)	NA
Control 2 Supine (5 ml) 1.0 *N* saline	4.2 (4.1–4.2)	4.5 (4.5–4.6)	4.5 (4.5–4.5)	NA
Control 2 Upright (5 ml) 0.5 *N* saline	6.5 (6.4–6.7)	4.0 (4.0–4.0)	4.2 (4.1–4.3)	NA
Control 2 Upright (5 ml) 1.0 *N* saline	5.1 (5.0–5.2)	4.4 (4.2–4.6)	4.8 (4.8–4.8)	NA
Control 2 Upright (30 ml) 0.5 *N* saline	21.5 (21.3–21.8)	4.3 (4.2–4.4)	4.1 (4.1–4.2)	NA

4D, four-dimensional; EGJ, esophagogastric junction.

Table 2. EGJ flow characteristics *versus* BFT, EII for Control 2. Median values and interquartile ranges are shown.

	4D manometry emptying time (s)	4D manometry bolus retention ratio	BFT (s)	EII
Supine (5 ml) 0.5 *N* saline	1.6 (1.2–2.2)	0.09 (0.07–0.12)	2.7 (2.2–3.1)	0.00 (0.00–0.08)
Supine (5 ml) 1.0 *N* saline	1.4 (1.3–1.5)	0.09 (0.09–0.09)	3.5 (3.1–3.8)	0.31 (0.30–0.31)
Upright (5 ml) 1 *N* saline	2.0 (1.8–2.2)	0.14 (0.11–0.16)	1.1 (0.5–1.6)	0.07 (0.04–0.11)
Upright (5 ml) 0.5 *N* saline	0.8 (0.8–0.8)	0.22 (0.15–0.30)	3.6 (2.0–5.1)	0.58 (0.29–0.87)
Upright (30 ml) 0.5 *N* saline	3.5 (3.3–3.8)	0.08 (0.06–0.10)	5.1 (5.0–5.1)	0.53 (0.48–0.58)

BFT, bolus flow time; 4D, four-dimensional; EGJ, esophagogastric junction; EII, esophageal impedance integral ratio.

Consequently, the mean flow rate (bolus volume reduction divided by emptying time), and the average emptying velocity (flow rate divided by EGJ CSA), were evaluated. DI was computed based on EGJ pressure and diameter during the emptying period and compared with that from the FLIP study.

Statistical analysis

The HRIM procedure on each subject includes tests in both supine and upright positions. Hence, for each HRIM study, we defined a subgroup as swallows of the same volume, the same concentration of saline, and the same body position. Within each subgroup, we computed medians and interquartile range (see Tables 1–3).

Results

Validations of 4D manometry calculations

Dynamics of bolus transit and calculated bolus volumes. Figure 1 illustrates the dynamics of bolus transit including the time-history of the total bolus volume and bolus retention volume (bottom) concurrent with pressure-impedance topography (top). For various swallow conditions

Table 3. Additional novel metrics of emptying from 4D manometry for Control 2 swallows. Median values and interquartile ranges are shown. Median DI is based on median EGJ pressure and emptying dimeter (i.e., 8 mm for 5 ml swallow, 10 mm for 30 ml swallow). For comparison, the Endoflip study of the same subject showed that DI at distension volume of 30, 40 and 50 ml was 2.3, 8.3 and 5.8 mm^2/mmHg, respectively.

	Maximum flow rate (ml/s)	Average flow rate (ml/s)	Maximum emptying velocity (cm/s)	Average emptying velocity (cm/s)	Median EGJ pressure (mmHg)	Median DI (mm^2/mmHg)
Supine (5 ml) 0.5 *N* saline	8.8 (7.8–10.4)	2.2 (1.9–2.7)	13.3 (11.1–14.2)	2.7 (2.1–3.9)	18.0 (16.9–20.5)	2.8 (2.5–3.0)
Supine (5 ml) 1.0 *N* saline	8.9 (8.3–9.5)	1.3 (1.3–1.4)	13.1 (12.1–14.2)	1.9 (1.6–2.1)	15.6 (15.2–16.0)	3.2 (3.1–3.3)
Upright (5 ml) 1.0 *N* saline	8.4 (8.1–8.7)	1.6 (1.6–1.6)	11.9 (11.6–12.1)	2.1 (2.1–2.1)	19.7 (19.4–20.0)	2.6 (2.5–2.6)
Upright (5 ml) 0.5 *N* saline	4.7 (4.7–4.7)	1.8 (1.8–1.8)	8.4 (8.4–8.4)	3.3 (3.3–3.3)	20.9 (20.9–2.9)	2.4 (2.4–2.4)
Upright (30 ml) 0.5 *N* saline	26.2 (25.9–26.6)	3.7 (3.4–3.9)	27.0 (26.8–27.1)	4.6 (4.3–5.0)	17.8 (17.0–18.6)	4.4 (4.2–4.6)

4D, four-dimensional; DI, distensibility index; EGJ, esophagogastric junction.

in Control 2 (Figure 1, panels 1–5), bolus intake occurred much more rapidly (<1.0 s) than emptying (>2.0 s). Minimal bolus retention was observed, except for an upright swallow of 5 ml 1.0 N supine (Figure 1, panel 4). For swallows in the Type-I Ach case, bolus retention and pre-swallow residual were observed as shown in Figure 1, panel 6. Table 1 shows the calculated *versus* actual bolus volume for Control 1 and Control 2 swallows. For 5 ml Control 2 swallows, the calculated bolus volumes ranged from 4.1 ml–6.7 ml, with most cases within 20% error. For 5 ml Control 1 swallows, greater variation was observed (3.2–5.8 ml), probably because the actual conductance of the barium-bolus mixture deviated from the assumed 8.12 mS/cm of 0.5 NS. If we work backward from the known swallowed bolus volume (i.e., 5 ml), and deduce the effective *in vivo* conductivity of bolus for Control 1 5 ml upright swallows, the actual *in vivo* conductivity of barium-based bolus could be estimated as around (3.6 ml/5.0 ml) * 8.12 mS/cm = 5.77 mS/cm. For the two 30 ml swallows, volume was under-predicted with an average error around 27%. The under prediction was likely because a 30-ml bolus was too large and a portion was likely retained in the mouth. Table 1 also illustrates the variability of calculated bolus volume with body position, although there was no consistent effect between subjects. Arguably, the current study showed that 4D manometry gave reasonable calculations of bolus volume, especially for standard 5 ml swallows. With a barium-based bolus, 4D manometry could deduce the actual conductivity of the *in vivo* bolus mixture that matched the nominal volume.

Timing and four phases against fluoroscopy. Figure 2 illustrates dynamic bolus transit based on simultaneous visualization of luminal morphology, impedance, and pressure with concurrent fluoroscopy images. The four phases of swallow can be delineated from the time-history of bolus transit. Phase I was esophageal filling, wherein impedance decreased and bolus volume in the body rapidly increased. The filling phase spanned from UES relaxation until UES tone was restored. The compartmentalization phase occurred for the next 3.5 s during which LES relaxation occurred as evident by the impedance and pressure measurement, but the bolus volume in the esophagus did not decrease. The esophageal emptying began once the bolus volume started to decrease at 3.8 s post swallow, initially rapid and then gradual. The initial fast emptying phase corresponded to 'esophageal emptying phase' driven by peristalsis, whereas the gradual emptying corresponded to 'ampullary emptying phase' driven by LES reconstitution. Interestingly, the onset of esophageal emptying coincided with peak bolus volume in the body and the onset of the distal esophageal contraction (i.e., the end of the transition zone). This coincidence was also observed in other swallows of normal controls and may have important physiological implications.

Type-I achalasia versus *normal.* All 10 swallow tests in the Type I Ach patient showed >4 ml bolus retention before and after the swallow. A typical case is shown in Figure 1, panel 6. Also characteristic of these swallows, the time-history

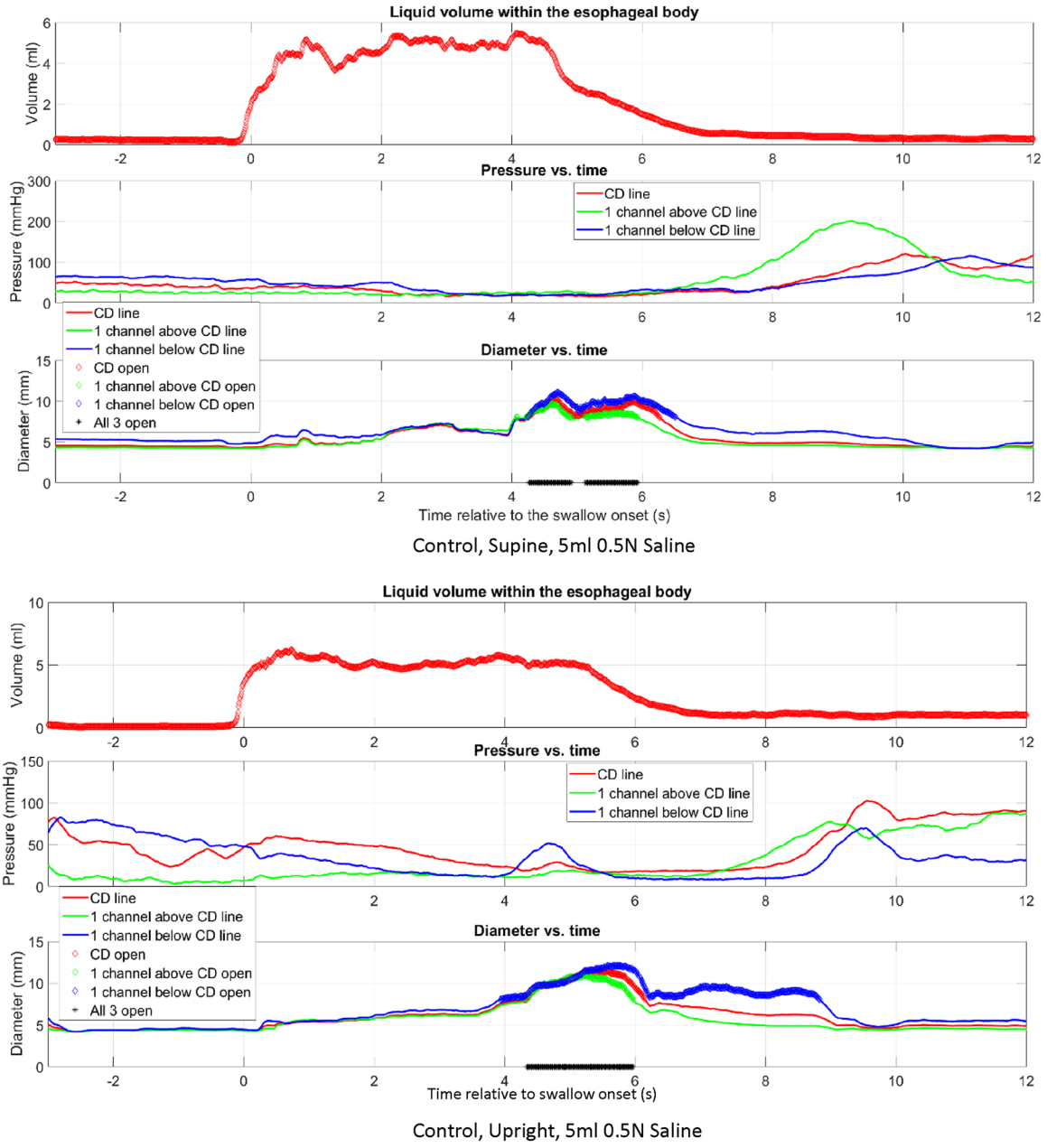

Figure 3. EGJ analysis of 5 ml swallows that delineate period of effective emptying. The concurrent plotting of bolus transit, EGJ pressure and diameters was used to delineate the period of effective esophageal emptying and evaluate DI listed in Table 3.
DI, distensibility index; EGJ, esophagogastric junction.

of bolus volume fluctuated due to the absence of an esophageal contraction and the delineation of four phases of bolus transit was obscured. Hence, the 4D manometry signature of Type I achalasia is the morphing of the time-history of pre-swallow bolus volume with post-swallow bolus retention.

EGJ analysis

EGJ emptying diameter: a threshold defines the effective esophageal emptying. Figure 3 (5 ml swallows from Control 2) and Figure 4 (Type-I Ach swallow and 30 ml swallow from Control 2) illustrate examples of simultaneous plots of bolus volume history, EGJ pressure, and EGJ diameter.

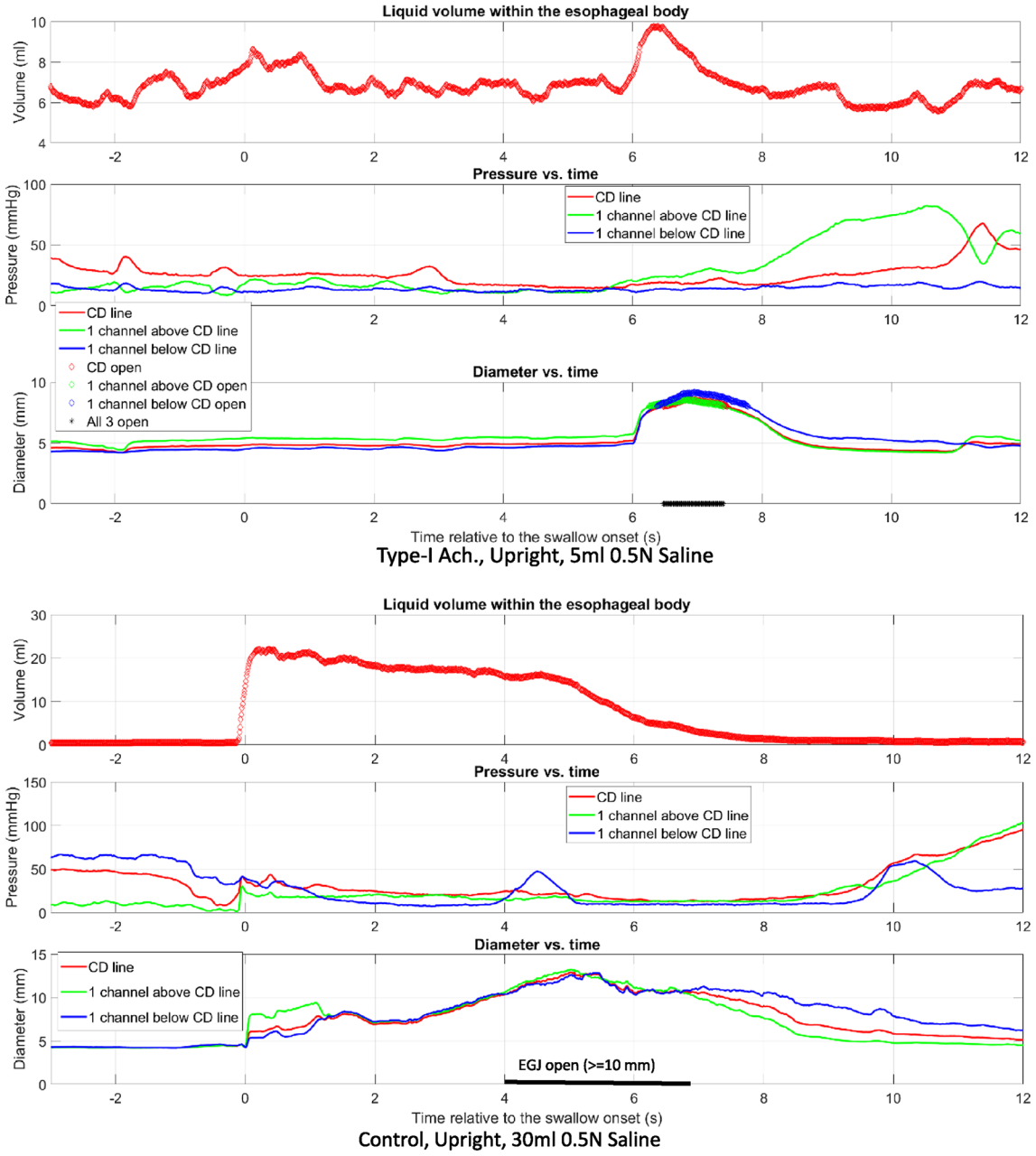

Figure 4. EGJ analysis of one swallow from Type-I Achalasia and one 30 ml swallow from Control 2. Concurrent plotting of bolus transit, EGJ pressure, and diameters was used to delineate the period of effective esophageal emptying and evaluate DI listed in Table 3 for a 30-ml swallow.
DI, distensibility index; EGJ, esophagogastric junction.

Esophageal emptying consistently occurred when the three EGJ diameters are ⩾8 mm for 5-ml swallows, and ⩾10 mm for 30-ml swallows suggesting these to be appropriate thresholds for delineating the period of 'effective esophageal emptying'. With the two criteria for esophageal emptying, one based on bolus volume and the other based on 'emptying diameter', the respective emptying onset times are shown in Table 1. For 5 of the 10 swallows, the time difference between the two criteria is around 0.4 s, which is small compared with a general 12 s window for a typical swallow. Table 2 also shows the onset time defined fluoroscopically on Control 1 which

exhibited a larger discrepancy of up to 1 s, likely attributable to the difficulty of discerning emptying onset fluoroscopically. Arguably, the proposed diameter-based criteria provided the most objective way to delineate the period of effective esophageal emptying.

EGJ-flow characteristics: 4D manometry versus *BFT; flow rate and distensibility.* Table 2 shows the 4D the EGJ flow characteristics that are comparable with BFT and EII ratio for Control 2. Specifically, 4D manometry emptying time, defined as the period of 'effective esophageal emptying' (see Figures 3 and 4) is analogues to the BFT. Compared with BFT analysis, the emptying time predicted by 4D manometry was more consistent among swallow types. Except for the 30 ml swallow and the upright swallow with 5 ml 0.5 N saline, the emptying time ranged from 1.2 s to 2.2 s. In contrast, the BFT ranged from 0.5 s to 3 s. Within the 4D manometry calculation, 30 ml swallows showed longer emptying time as expected, whereas upright swallow did not necessarily lead to shorter emptying time. An analogue to the E-II ratio is the bolus retention ratio, defined as maximal retention volume divided by the normal bolus volume. For all Control 2 swallows, the bolus retention ratio was consistently minimal (<0.1 in most of cases) in contrast with the EII, which ranged from 0.08 to 0.58. For the Type I Ach case, all swallows, except the one showed in Figure 4, panel 1, showed no effective esophageal emptying. Figure 4, panel 1 shows a very short period of emptying, followed by LES restoration leaving a large amount of retention (see also Figure 1, panel 6).

Additional novel metrics of emptying calculated by 4D manometry are shown in Table 3. For 5 ml swallows, average flow rate ranged from 1.3 to 2.7 ml/s, whereas the maximal flow rate was as high as 10.5 ml/s, likely occurring at the very beginning of emptying. The median EGJ pressure ranged from 15 to 20 mmHg and the EGJ DI ranged from 2.4 to 3.4 mm^2/mmHg for 5 ml swallows and 4.2–4.6 mm^2/mmHg for 30 ml swallows, respectively. A greater DI for 30 ml swallow is expected due to a larger emptying diameter and these values are more consistent with DI measured from FLIP study of the same subject, which showed DI of 2.3 mm^2/mmHg at 30 ml distension volume, and DI = 5.8 mm^2/mmHg at the 50 ml volume.

Discussion

In this work, we describe a analytic methodology, 4D manometry, for post-processing HRIM data to dynamically characterize and visualize esophageal luminal geometry, contractility, and bolus transport during test swallows. Compared with conventional manometry, 4D manometry provides a comprehensive characterization of temporal-spatial dynamics of bolus transit (see supplemental movies). This approach facilitates quantification of bolus flow within and through the esophagus as well as visualizing and quantifying esophageal wall distensibility. Furthermore, 4D manometry requires minimal additional information for HRIM post-processing. Specifically, if only the swallow bolus volume is known, the current method can even deduce an effective bolus resistance *in vivo*, as illustrated in Appendix Equation (7).

The current work is not the first study to construct esophageal luminal geometry from impedance measurement. FLIP is a related technique that uses impedance sensors within a cylindrical bag filled with conductive fluid to CSA measurements. However, with respect to motility the current FLIP procedure has only a single pressure sensor and is used primarily to assess secondary peristalsis. More analogous to the current study, Kim *et al.* used HRIM impedance data with concurrent ultrasound imaging of the esophageal wall to study the correlation between luminal CSA and impedance change describing a qualitative inverse relationship between impedance and peak CSA.[14] Zifan *et al.* proposed a methodology to quantify CSA from impedance data, which required swallowing boluses of two different conductivity values in order to derive tissue conductivity.[15] With that method, they investigated contraction-distention topography along the entire esophagus during peristalsis assisted with the ultrasound.[16] The current 4D manometry differs from these previous approaches in several ways. First, it relies only on standard HRIM measurements of each swallow as long as the bolus volume or conductivity is known. This provides great applicability of 4D manometry to post-processing existing HRIM data. In particular, with known swallow bolus volume, the current method can circumvent the challenge of measuring bolus conductivity *in vivo*, which may differ from *in vitro* conductivity due to mixing between the bolus luminal fluids. Second, the

proposed 4D manometry provides more comprehensive and innovate metrics of esophageal morphology and bolus transport within the body and through the EGJ. Specifically, 4D manometry provides concurrent spatial-temporal representations of luminal geometry and pressure, and the time-history of bolus volume and bolus retention volume during peristalsis. Subsequent EGJ analysis enables the quantification of emptying time, mean bolus velocity, flow rate as well as EGJ DI. In overall, the range of EGJ DI values calculated with 4D manometry were very similar to the EGJ DI values calculated using FLIP in asymptomatic controls,[10] but certain discrepancies between DI from 4D manometry and FLIP are also observed. In particular, at volume of 30 ml, DI from 4D manometry is greater than DI from FLIP (4.4 *versus* 2.3). This is likely related to the difference of EGJ physiology during normal emptying in the 4D manometry analysis and that measured during volume-based dilation in FLIP when esophageal distention is likely stimulating contraction.

BFT and EII-ratio are other metrics developed to illustrate bolus retention and flow based on impedance data. Compared with EII-ratio, 4D manometry provides a more quantitative evaluation of bolus retention including its time-history and an overview of dynamic bolus transit. In comparison with the BFT, 4D manometry calculates the period of effective esophageal emptying from impedance data only circumventing the difficulty of artifact pressure transients attributable to contact between EGJ wall and the pressure sensors.

Validations of 4D manometry in the current study found reasonable correlation between calculated and actual bolus volume, but the error was not small in some cases. Potential sources of this error include: (1) change of effective conductivity of the bolus due to *in vitro* dilution, (2) approximation error from assuming a circular luminal shape, and (3) catheter or EGJ axial movement. The first two factors are expected to be the dominant ones, whereas the third factor could be corrected by visual inspection of the pressure topography. In instance of known bolus volume, the first factor can also be fixed using the deduced effective bolus conductivity based on Appendix Equation (7). Zifan *et al.* mentioned another potential source of error related to luminal air which has two aspects, its effect on conductance [Equation (1)] and its effect on luminal CSA. The effect on conductance can be safely ignored, as the conductivity of air ($\sim 10^{-9}$ S/m) is about seven orders of magnitude greater than that of drinking water or saline ($\sim 10^{-2}$ S/m). The influence of air on luminal CSA can be sorted out by *always* interpreting the calculated luminal CSA as that of the swallowed bolus (i.e., liquid CSA).

As a preliminary study, one limitation of the current work is the small number of cases included. More studies with comprehensive measurements from both HRIM and fluoroscopy could help to refine several outcomes. However, this would require a fairly complicated procedure of HRIM synchronized with a concurrent fluoroscopy that we are currently unable to conduct. Consequently, this preliminary study illustrates a new analysis algorithm, and we plan on studying larger cohorts of patients and controls in future work.

In summary, the proposed 4D manometry tool, based on simple biophysical analysis, enables a comprehensive characterization of temporal-spatial dynamics of esophageal bolus transit with concurrent pressure and luminal geometry. Further biomechanical analysis can deduce additional metrics such as the flow rate, esophageal wall distensibility, and esophageal retention. The methodology was validated against volume predictions on fluoroscopy, and the DI prediction from Endoflip. Preliminary studies showed 4D manometry could easily differentiate normal from Type I Achalasia, which featured pre- and post-swallow residual and minimal EGJ opening. Large cohort studies will be conducted in future to determine whether 4D manometry can further refine motility diagnoses that are currently heterogeneous such as ineffective esophageal motility and EGJ outflow obstruction.

Author contributions

WK and JEP contributed to study concept and design, data analysis. WK, DAC, NAP, JEP, and PJK contributed data interpretation, drafting of the manuscript, and approval of the final version.

Conflict of interest statement

Wenjun Kou: Crospon, Inc. (Consulting)

Neelesh A. Patankar and Peter J. Kahrilas disclose no conflicts of interest

Dustin A. Carlson and John E. Pandolfino hold shared intellectual property rights and ownership

surrounding FLIP panometry systems, methods, and apparatus with Medtronic Inc.

Dustin A. Carlson: Medtronic (speaking, consulting)

John E. Pandolfino: Crospon, Inc (stock options), Given Imaging (consultant, grant, speaking), Sandhill Scientific (consulting, speaking), Takeda (speaking), Astra Zeneca (speaking), Medtronic (speaking, consulting), Torax (speaking, consulting), Ironwood (consulting), Impleo (grant).

Funding

The authors disclosed receipt of the following financial support for the research, authorship, and/or publication of this article: This work was supported by P01 DK117824 (JEP) from the Public Health service.

ORCID iD

Wenjun Kou https://orcid.org/0000-0003-2582-2070

Supplemental material

Supplemental material for this article is available online.

References

1. Ghosh SK, Janiak P, Schwizer W, *et al.* Physiology of the esophageal pressure transition zone: separate contraction waves above and below. *Am J Physiol Gastrointest Liver Physiol* 2006; 290: G568–G576.
2. Kou W, Griffith BE, Pandolfino JE, *et al.* A continuum mechanics-based musculo-mechanical model for esophageal transport. *J Comput Phys* 2017; 348: 433–459.
3. Kou W, Pandolfino JE, Kahrilas PJ, *et al.* Simulation studies of circular muscle contraction, longitudinal muscle shortening, and their coordination in esophageal transport. *Am J Physiol Gastrointest Liver Physiol* 2015; 309: G238–G247.
4. Kahrilas PJ, Bredenoord AJ, Fox M, *et al.* The Chicago classification of esophageal motility disorders, v3.0. *Neurogastroenterol Motil* 2015; 27: 160–174.
5. Mittal RK, Padda B, Bhalla V, *et al.* Synchrony between circular and longitudinal muscle contractions during peristalsis in normal subjects. *Am J Physiol Gastrointest Liver Physiol* 2006; 290: G431–G438.
6. Lin Z, Yim B, Gawron A, *et al.* The four phases of esophageal bolus transit defined by high-resolution impedance manometry and fluoroscopy. *Am J Physiol Gastrointest Liver Physiol* 2014; 307: G437–G444.
7. Pandolfino JE, Zhang QG, Ghosh SK, *et al.* Transient lower esophageal sphincter relaxations and reflux: mechanistic analysis using concurrent fluoroscopy and high-resolution manometry. *Gastroenterology* 2006; 131: 1725–1733.
8. Goldberg MF, Levine MS and Torigian DA. Diffuse esophageal spasm: CT findings in seven patients. *AJR Am J Roentgenol* 2008; 191: 758–763.
9. Miyazaki Y, Nakajima K, Sumikawa M, *et al.* Magnetic resonance imaging for simultaneous morphological and functional evaluation of esophageal motility disorders. *Surg Today* 2014; 44: 668–676.
10. Carlson DA, Kou W, Lin Z, *et al.* Normal values of esophageal distensibility and distension-induced contractility measured by functional luminal imaging probe panometry. *Clin Gastroenterol Hepatol* 2019; 17: 674–681.e671.
11. Carlson DA, Lin Z, Rogers MC, *et al.* Utilizing functional lumen imaging probe topography to evaluate esophageal contractility during volumetric distention: a pilot study. *Neurogastroenterol Motil* 2015; 27: 981–989.
12. Carlson DA, Lin Z, Kou W, *et al.* Inter-rater agreement of novel high-resolution impedance manometry metrics: bolus flow time and esophageal impedance integral ratio. *Neurogastroenterol Motil* 2018; 30: e13289.
13. Lin Z, Imam H, Nicodème F, *et al.* Flow time through esophagogastric junction derived during high-resolution impedance-manometry studies: a novel parameter for assessing esophageal bolus transit. *Am J Physiol Gastrointest Liver Physiol* 2014; 307: G158–G163.
14. Kim JH, Mittal RK, Patel N, *et al.* Esophageal distension during bolus transport: can it be detected by intraluminal impedance recordings? *Neurogastroenterol Motil* 2014; 26: 1122–1130.
15. Zifan A, Ledgerwood-Lee M and Mittal RK. Measurement of peak esophageal luminal cross-sectional area utilizing nadir intraluminal impedance. *Neurogastroenterol Motil* 2015; 27: 971–980.
16. Zifan A, Song HJ, Youn YH, *et al.* Topographical plots of esophageal distension and contraction: effects of posture on esophageal peristalsis and bolus transport. *Am J Physiol Gastrointest Liver Physiol* 2019; 316: G519–G526.